Compactly Supported Tensor Product Complex Tight Framelets with Directionality

Xiaosheng Zhuang
Department of Mathematics, City University of Hong Kong, Tat Chee Avenue, Kowloon Tong, Hong Kong
Email: xzhuang7@cityu.edu.hk
Bin Han
Department of Mathematical and Statistical Sciences, University of Alberta,Edmonton, Alberta, Canada T6G 2G1
Email: bhan@ualberta.ca

***Abstract*—Construction of directional compactly supported tensor product complex tight framelets $\mathrm{cptTP\text{-}\mathbb{C}TF}_6$ is discussed. The construction algorithm employs optimization techniques and puts extensive emphasis on frequency response and spatial localization of the underlying one-dimensional tight framelet filter banks. A concrete example of $\mathrm{cptTP\text{-}\mathbb{C}TF}_6$ is provided. Numerical experiments show that such constructed $\mathrm{cptTP\text{-}\mathbb{C}TF}_6$ have good performance in image denoising.**

I. Introduction

To achieve directionality for multidimensional problems, by using complex-valued high-pass filters in a tight framelet filter bank, recently a family of directional tensor product complex tight framelets $\mathrm{TP\text{-}\mathbb{C}TF}_n$ with $n \geqslant 3$ has been introduced in [10] and further developed in [13], [14], where n is the total number of filters in the underlying one-dimensional tight framelet filter banks. Experimental results demonstrate that tensor product complex tight framelets, especially $\mathrm{TP\text{-}\mathbb{C}TF}_6$, have significantly better performance than many other transform-based methods for the model problems of image denoising in [13], image inpainting in [25], and video denoising/inpainting in [14]. However, the tensor product complex tight framelets constructed in [10], [13], [14] are band-limited, that is, they are compactly supported in the frequency domain. Hence, in the spatial/time domain, they cannot have compact support. Since compactly supported wavelets or framelets have good space-frequency localization and lead to efficient computational algorithms, they are of great importance both theoretically and practically. The initial effort on finding directional compactly supported tensor product complex tight framelets $\mathrm{cptTP\text{-}\mathbb{C}TF}_n$ has been started in [12], which concentrates on the simplest directional compactly supported $\mathrm{cptTP\text{-}\mathbb{C}TF}_3$ with only two high-pass filters in one dimension.

In this paper we are interested in constructing directional compactly supported tensor product complex tight framelets, $\mathrm{cptTP\text{-}\mathbb{C}TF}_6$, with good performance for applications such as image denoising. In the following sections, we first briefly review tensor product tight framelets and recall the construction of the band-limited tensor product complex tight framelet filter banks $\mathrm{TP\text{-}\mathbb{C}TF}_n$ with $n \geqslant 3$. We then discuss the filters' frequency separation property and provide a step-by-step algorithm for constructing compactly supported $\mathrm{cptTP\text{-}\mathbb{C}TF}_6$ having good frequency separation property with prescribed filter supports. Finally, we test the constructed $\mathrm{cptTP\text{-}\mathbb{C}TF}_6$ in image denoising.

II. Tensor Product Tight Framelets

By $u \in l_0(\mathbb{Z}^d)$ we mean that u is a sequence on $\mathbb{Z}^d$ having finite support. For $1 \leqslant p < \infty$, we say that $u = \{u(k)\}_{k\in\mathbb{Z}^d} \in l_p(\mathbb{Z}^d)$ if $\|u\|^p_{l_p(\mathbb{Z}^d)} := \sum_{k\in\mathbb{Z}^d} |u(k)|^p < \infty$. For $u = \{u(k)\}_{k\in\mathbb{Z}^d} \in l_2(\mathbb{R}^d)$, we define its *Fourier series* (or symbol) to be $\widehat{u}(\xi) := \sum_{k\in\mathbb{Z}^d} u(k)e^{-ik\cdot\xi}$, $\xi \in \mathbb{R}^d$.

For $a, b_1, \ldots, b_s \in l_2(\mathbb{R}^d)$, we say that $\{a; b_1, \ldots, b_s\}$ is a (d-dimensional dyadic) *tight framelet filter bank* if

$$\widehat{a}(\xi)\overline{\widehat{a}(\xi+\pi\omega)} + \sum_{\ell=1}^{s} \widehat{b_\ell}(\xi)\overline{\widehat{b_\ell}(\xi+\pi\omega)} = \delta_\omega,$$

for $\omega \in ([0,1]^d \cap \mathbb{Z}^d)$ and for almost every $\xi \in \mathbb{R}^d$.

If there exist positive numbers C and τ such that $|\widehat{a}(\xi) - 1| \leqslant C|\xi|^\tau$ for all $\xi \in [-\pi,\pi]^d$ (this condition is automatically satisfied if $a \in l_0(\mathbb{Z}^d)$ and $\widehat{a}(0) = 1$), then the following functions are well defined for a tight framelet filter bank $\{a; b_1, \ldots, b_s\}$:

$$\widehat{\phi}(\xi) := \prod_{j=1}^{\infty} \widehat{a}(2^{-j}\xi) \text{ and } \widehat{\psi_\ell}(\xi) := \widehat{b_\ell}(\xi/2)\widehat{\phi}(\xi/2),$$

$\xi \in \mathbb{R}^d$, $\ell = 1, \ldots, s$, where the *Fourier transform* is defined to be $\widehat{f}(\xi) := \int_{\mathbb{R}^d} f(x)e^{-ix\cdot\xi}dx$ for $f \in L_1(\mathbb{R}^d)$. Then it is known in [9, Theorem 17 and Corollary 12] that $\{\phi; \psi_1, \ldots, \psi_s\}$ is a *tight framelet* for $L_2(\mathbb{R}^d)$, that is,

$$\|f\|^2_{L_2(\mathbb{R}^d)} = \sum_{k\in\mathbb{Z}^d} |\langle f, \phi(\cdot - k)\rangle|^2 + \sum_{j=0}^{\infty}\sum_{\ell=1}^{s}\sum_{k\in\mathbb{Z}^d} |\langle f, 2^{dj/2}\psi^\ell(2^j\cdot - k)\rangle|^2, \ \forall f \in L_2(\mathbb{R}^d).$$

If $a \in l_0(\mathbb{Z}^d)$ with $\widehat{a}(0) = 1$, then $\{\phi; \psi_1, \ldots, \psi_s\}$ is a tight framelet for $L_2(\mathbb{R}^d)$ if and only if $\{a; b_1, \ldots, b_s\}$ is a tight framelet filter bank. As a consequence, in this paper we mainly concentrate on tight framelet filter banks instead of tight framelets for $L_2(\mathbb{R}^d)$.

A d-dimensional dyadic tight framelet filter bank can be easily obtained through the tensor product of a one-dimensional tight framelet filter bank. For filters $u_1, \ldots, u_d \in l_1(\mathbb{Z})$ in

one dimension, we define their d-dimensional tensor product filter $u_1 \otimes \cdots \otimes u_d$ to be $(u_1 \otimes \cdots \otimes u_d)(k_1, \ldots, k_d) := u_1(k_1) \cdots u_d(k_d)$ for $k_1, \ldots, k_d \in \mathbb{Z}$. In particular, we define $\otimes^d u := u \otimes \cdots \otimes u$ as the tensor product of d copies of u. If $\{a; b_1, \ldots, b_s\}$ is a one-dimensional tight framelet filter bank, then it is straightforward to check that $\otimes^d\{a; b_1, \ldots, b_s\} := \{h_1 \otimes \cdots \otimes h_d : h_j \in \{a; b_1, \ldots, b_s\}, j = 1, \ldots, d\}$ is a d-dimensional tight framelet filter bank with the d-dimensional low-pass filter $\otimes^d a$.

III. Band-limited Tensor Product Complex Tight Framelets TP-$\mathbb{C}$TF$_n$

We now briefly recall the construction of band-limited tensor product complex tight framelets in [10], [13], [14]. For $c_L < c_R$ and two positive numbers ε_L, ε_R satisfying $\varepsilon_L + \varepsilon_R \leqslant c_R - c_L$, let $\chi_{[c_L, c_R]; \varepsilon_L, \varepsilon_R}$ on $\mathbb{R}$ be a bump function defined as in [14, (3.1)], which is supported on $[c_L - \varepsilon_L, c_R + \varepsilon_R]$. Let $s \in \mathbb{N}$ and $0 < c_1 < c_2 < \cdots < c_{s+1} := \pi$ and $\varepsilon_0, \varepsilon_1, \ldots, \varepsilon_{s+1}$ be positive real numbers satisfying $0 < \varepsilon_0 < c_1 - \varepsilon_1$, $0 < \varepsilon_1 \leqslant \min(c_1, \frac{\pi}{2} - c_1)$, $(c_{\ell+1} - c_\ell) + \varepsilon_{\ell+1} + \varepsilon_\ell \leqslant \pi$, $\ell = 1, \ldots, s$. The filters $a, a^+, a^-, b_1^+, \ldots, b_s^+, b_1^-, \ldots, b_s^-$ are defined through their 2π-periodic Fourier series on the basic interval $[-\pi, \pi)$ as:

$$\begin{aligned} \widehat{a} :=& \chi_{[-c_1, c_1]; \varepsilon_1, \varepsilon_1},\ \widehat{a^+} := \chi_{[0, c_1]; \varepsilon_0, \varepsilon_1},\ \widehat{a^-} := \overline{\widehat{a^+}(-\cdot)}, \\ \widehat{b_\ell^+} :=& \chi_{[c_\ell, c_{\ell+1}]; \varepsilon_\ell, \varepsilon_{\ell+1}},\ \widehat{b_\ell^-} := \overline{\widehat{b_\ell^+}(-\cdot)}, \quad \ell = 1, \ldots, s. \end{aligned}$$

Then $\mathbb{C}\mathrm{TF}_{2s+1} := \{a; b_1^+, \ldots, b_s^+, b_1^-, \ldots, b_s^-\}$ and $\mathbb{C}\mathrm{TF}_{2s+2} := \{a^+, a^-; b_1^+, \ldots, b_s^+, b_1^-, \ldots, b_s^-\}$ are (one-dimensional dyadic) tight framelet filter banks. The *tensor product complex tight framelet filter banks* TP-$\mathbb{C}\mathrm{TF}_{2s+1}$ and TP-$\mathbb{C}\mathrm{TF}_{2s+2}$ in d dimensions are given by

$$\begin{aligned} &\text{TP-}\mathbb{C}\mathrm{TF}_{2s+1} := \otimes^d\{a; b_1^+, \ldots, b_s^+, b_1^-, \ldots, b_s^-\}, \\ &\text{TP-}\mathbb{C}\mathrm{TF}_{2s+2} := \{\otimes^d a\} \cup \left(\otimes^d \mathbb{C}\mathrm{TF}_{2s+2} \setminus \otimes^d \{a^+, a^-\}\right). \end{aligned}$$

See [10], [12]–[14], [25] for detailed discussions on tensor product complex tight framelets and their applications to image/video processing.

IV. Construction of Compactly Supported Tensor Product Complex Tight Framelets cptTP-$\mathbb{C}$TF$_6$

The above constructed TP-$\mathbb{C}\mathrm{TF}_n$ with $n \geqslant 3$ are band-limited and do not have compact support in the spatial domain. Due to the importance of *compactly supported tensor product complex tight framelets* (cptTP-$\mathbb{C}\mathrm{TF}_n$) in both theory and application, it is highly desirable to know whether it is possible to construct directional cptTP-$\mathbb{C}\mathrm{TF}_n$ with good performance in practical applications over other state-of-the-art transform-based methods in the literature.

As explained in [12]–[14], the directionality of TP-$\mathbb{C}\mathrm{TF}_n$ with $n \geqslant 3$ in high dimensions is mainly due to the following frequency separation property:

$$\widehat{b_\ell^+}(\xi) \approx 0,\ \xi \in [-\pi, 0] \quad \text{or} \quad \widehat{b_\ell^-}(\xi) \approx 0,\ \xi \in [0, \pi], \tag{1}$$

$\ell = 1, \ldots, s$. That is, all $\widehat{a^+}, \widehat{b_1^+}, \ldots, \widehat{b_s^+}$ nearly vanish on $[-\pi, 0]$ and mostly concentrate on $[0, \pi]$, while all $\widehat{a^-}, \widehat{b_1^-}, \ldots, \widehat{b_s^-}$ nearly vanish on $[0, \pi]$ and mostly concentrate on $[-\pi, 0]$. In view of (1), when consider compactly supported framelets, for their associated finitely supported filters $b = \{b(k)\}_{k \in \mathbb{Z}} \in l_0(\mathbb{Z})$ which is not identically zero, we introduce the following quantity to measure *frequency separation* of the filter b:

$$\mathrm{fsp}(b) := \frac{\min\left\{\frac{1}{\pi}\int_{-\pi}^0 |\widehat{b}(\xi)|^2 d\xi, \frac{1}{\pi}\int_0^\pi |\widehat{b}(\xi)|^2 d\xi\right\}}{\frac{1}{2\pi}\int_{-\pi}^\pi |\widehat{b}(\xi)|^2 d\xi}. \tag{2}$$

It is straightforward to observe that $0 \leqslant \mathrm{fsp}(b) \leqslant 1$. The smaller the quantity $\mathrm{fsp}(b)$ is, the better the frequency separation of the filter b will have. If b is a real-valued filter, then $\widehat{b}(\xi) = \overline{\widehat{b}(-\xi)}$ and we can check that $\mathrm{fsp}(b) = 1$. However, things can be quite different for complex-valued filters. Define a sequence $c = \{c(k)\}_{k \in \mathbb{Z}}$ by $\widehat{c}(\xi) := |\widehat{b}(\xi)|^2$. The quantity $\mathrm{fsp}(b)$ in (2) can be easily computed by $\mathrm{fsp}(b) = 1 - \frac{4|C_b|}{\pi c(0)}$ with $C_b := \mathrm{Im}\left(\sum_{j=1}^\infty \frac{c(2j-1)}{2j-1}\right)$, since $\frac{1}{2\pi}\int_{-\pi}^\pi |\widehat{b}(\xi)|^2 d\xi = c(0) = \|b\|_{l_2(\mathbb{Z})}^2$, $\frac{1}{\pi}\int_{-\pi}^0 |\widehat{b}(\xi)|^2 d\xi = c(0) + \frac{4C_b}{\pi}$, and $\frac{1}{\pi}\int_0^\pi |\widehat{b}(\xi)|^2 d\xi = c(0) - \frac{4C_b}{\pi}$.

For any tight framelet filter bank $\{a; b^+, b^-\}$ with $b^- = \overline{b^+}$, [12, Theorem 1] says

$$\mathrm{fsp}(b^+) = \mathrm{fsp}(b^-) \geqslant \frac{\frac{1}{\pi}\int_0^\pi A(\xi) d\xi}{1 - \|a\|_{l_2(\mathbb{Z})}^2} =: \mathrm{fsp}(a \,|\, \mathrm{hp}), \tag{3}$$

where hp in $\mathrm{fsp}(a \,|\, \mathrm{hp})$ stands for high-pass and

$$A(\xi) := \frac{1}{2}\left(1 - B(\xi) - \sqrt{4B(\xi) + C(\xi)}\right), \tag{4}$$

with $B(\xi) := 1 - |\widehat{a}(\xi)|^2 - |\widehat{a}(\xi + \pi)|^2$ and $C(\xi) = |\widehat{a}(\xi)|^2 - |\widehat{a}(\xi + \pi)|^2$.

For splitting a real-valued filter a into two auxiliary filters a^+ and a^- with $a^- = \overline{a^+}$ and preserving the tightness property of the filter bank $\{a^\pm; b_1^\pm, \ldots, b_s^\pm\}$, similarly, one can show that

$$\mathrm{fsp}(a^+) = \mathrm{fsp}(a^-) \geqslant \mathrm{fsp}(a \,|\, \mathrm{lp}), \tag{5}$$

where $\mathrm{fsp}(a \,|\, \mathrm{lp}) := \frac{\frac{1}{\pi}\int_0^\pi \min(|\widehat{a}(\xi)|^2, |\widehat{a}(\xi+\pi)|^2) d\xi}{\|a\|_{l_2(\mathbb{Z})}^2}$ and lp in $\mathrm{fsp}(a \,|\, \mathrm{lp})$ stands for low-pass. Note that $0 \leqslant \mathrm{fsp}(a \,|\, \mathrm{lp}) \leqslant 1$.

We now present in Algorithm 1 the construction of cptTP-$\mathbb{C}\mathrm{TF}_6$ with good frequency separation property, which we briefly summarize here: The steps (S1)–(S3) focus on splitting a low-pass filter $a \in l_0(\mathbb{Z})$ into two auxiliary finitely supported low-pass filters a^+, a^- with good frequency separation. Note that $\widehat{a^-}(\xi) = \overline{\widehat{a^+}(-\xi)}$ and $\widehat{a^+}, \widehat{a^-}$ are 2π-periodic. Hence (S3) minimizes the 'energy' of $\widehat{a^+}$ in $[-\pi, 0]$ and $\widehat{a^-}$ in $[0, \pi]$. The steps (S4)–(S5) then build finitely supported high-pass filters $b_1^+, b_1^-, b_2^+, b_2^-$ so that the filter bank $\{a^+, a^-; b_1^+, b_1^-, b_2^+, b_2^-\} \subset l_0(\mathbb{Z})$ has good frequency separation property similar to the band-limited $\mathbb{C}\mathrm{TF}_6$ in [13], [14].

Algorithm 1. *Let $a \in l_0(\mathbb{Z})$ be a real-valued filter on $\mathbb{Z}$ satisfying $|\widehat{a}(\xi)|^2 + |\widehat{a}(\xi + \pi)|^2 \leqslant 1$ for all $\xi \in \mathbb{R}$.*

(S1) *Choose an integer* $M \in \mathbb{N} \cup \{0\}$ *and define*

$$\begin{bmatrix} \mathsf{u}_1(\xi) & \mathsf{u}_2(\xi) \\ \mathsf{u}_3(\xi) & \mathsf{u}_4(\xi) \end{bmatrix} := \begin{bmatrix} \cos(t_0) & -\sin(t_0) \\ \sin(t_0) & \cos(t_0) \end{bmatrix} \prod_{j=1}^{M} \begin{bmatrix} \cos(t_j) & -\sin(t_j) \\ e^{-i\xi}\sin(t_j) & e^{-i\xi}\cos(t_j) \end{bmatrix},$$

where $t_0, \ldots, t_M \in [-\pi, \pi]$ *are real numbers to be determined later.*

(S2) *Define two filters* a^+ *and* a^- *by* $\widehat{a^+}(\xi) := \widehat{a}(\xi)\widehat{u^+}(2\xi)$ *and* $\widehat{a^-}(\xi) := \widehat{a}(\xi)\widehat{u^-}(2\xi)$*, where*

$$\widehat{u^+}(\xi) := \frac{1}{\sqrt{2}}[\mathsf{u}_1(\xi) + i\mathsf{u}_2(\xi)],\ \widehat{u^-}(\xi) := \frac{1}{\sqrt{2}}[\mathsf{u}_1(\xi) - i\mathsf{u}_2(\xi)].$$

(S3) *Find a solution* $\{t_0, \ldots, t_M\}$ *of the following optimization problem:*

$$\min_{t_0,\ldots,t_M} \int_0^\pi \left(|\widehat{a^+}(\xi+\pi)|^2 + |\widehat{a^-}(\xi)|^2 \right) d\xi.$$

(S4) *Choose a suitable integer* $N \in \mathbb{N} \cup \{0\}$ *and parameterize high-pass filters* b_1^+ *and* b_2^+ *by*

$$\widehat{b_1^+}(\xi) := s_0 + s_1 e^{-i\xi} + \cdots + s_N e^{-iN\xi},$$
$$\widehat{b_2^+}(\xi) := c_0 + c_1 e^{-i\xi} + \cdots + c_N e^{-iN\xi},$$

where $s_0, \ldots, s_N, c_0, \ldots, c_N$ *are complex numbers to be determined later. Define* b_1^-, b_2^- *through* $\widehat{b_1^-} = \overline{\widehat{b_1^+}(-\cdot)}$ *and* $\widehat{b_2^-} = \overline{\widehat{b_2^+}(-\cdot)}$.

(S5) *Find a solution* $\{s_0, \ldots, s_N, c_0, \ldots, c_N\}$ *of complex numbers to the following constrained optimization problem:*

$$\min_{\substack{s_k, c_k \\ k=0,\ldots,N}} \lambda_1 I_1 + \lambda_2 I_2 - \lambda_3 I_3 - \lambda_4 I_4,$$

under the constraints for a tight framelet filter bank $\{a; b_1^+, b_2^+, b_1^-, b_2^-\}$:

$$|\widehat{b_1^+}(\xi)|^2 + |\widehat{b_2^+}(\xi)|^2 + |\widehat{b_1^-}(\xi)|^2 + |\widehat{b_2^-}(\xi)|^2 = 1 - |\widehat{a}(\xi)|^2,$$
$$\sum_{\ell=1}^{2} \left(\widehat{b_\ell^+}(\xi)\overline{\widehat{b_\ell^+}(\xi+\pi)} + \widehat{b_\ell^-}(\xi)\overline{\widehat{b_\ell^-}(\xi+\pi)} \right) = -\widehat{a}(\xi)\overline{\widehat{a}(\xi+\pi)},$$

for all $\xi \in \mathbb{R}$*, where*

$$I_1 = \int_{\frac{\pi}{4}}^{\frac{7\pi}{12}} |\widehat{b_1^+}(\xi)|^2 d\xi, \quad I_2 = \int_{\frac{\pi}{2}}^{\frac{5\pi}{6}} |\widehat{b_2^-}(\xi)|^2 d\xi,$$
$$I_3 = \int_{-\frac{\pi}{2}}^{-\frac{\pi}{6}} |\widehat{b_1^+}(\xi)|^2 d\xi, \quad I_4 = \int_{-\frac{3\pi}{4}}^{-\frac{5\pi}{12}} |\widehat{b_1^-}(\xi)|^2 d\xi.$$

(such constraints on b_1^+*,* b_2^+*,* b_1^-*, and* b_2^- *can be rewritten as equations in terms of* $s_0, \ldots, s_N, c_0, \ldots, c_N$*), where* $\lambda_1, \ldots, \lambda_4$ *are real positive regularization parameters.*

Then $\mathbb{C}\mathrm{TF}_6 := \{a^+, a^-; b_1^+, b_2^+, b_1^-, b_2^-\}$ *is a finitely supported tight framelet filter bank with small frequency separation quantities* $\mathrm{fsp}(a^+)$*,* $\mathrm{fsp}(b_1^+)$*, and* $\mathrm{fsp}(b_2^+)$*.*

To illustrate Algorithm 1 we present one concrete example. We set the regularization parameters $\lambda_1 = 2.2, \lambda_2 = 1, \lambda_3 = 0, \lambda_4 = -2.5$ for Algorithm 1. We use a numerical routine in the computer algebra software MAPLE to solve the optimization problems in (S3) and (S5) of Algorithm 1.

Example 1. Consider a low-pass filter a as follows:

$$a = \Big\{ \tfrac{1+\sqrt{28}}{256} - \tfrac{\sqrt{8+2\sqrt{28}}}{256}, \tfrac{1+\sqrt{7}}{32} - \tfrac{3\sqrt{8+2\sqrt{28}}}{128}, \tfrac{7+\sqrt{28}}{64} - \tfrac{7\sqrt{8+2\sqrt{28}}}{128},$$
$$\tfrac{7-\sqrt{7}}{32} - \tfrac{7\sqrt{8+2\sqrt{28}}}{128}, \tfrac{35-5\sqrt{28}}{128}, \tfrac{7-\sqrt{7}}{32} + \tfrac{7\sqrt{8+2\sqrt{28}}}{128},$$
$$\tfrac{7+\sqrt{28}}{64} + \tfrac{7\sqrt{8+2\sqrt{28}}}{128}, \tfrac{1+\sqrt{7}}{32} + \tfrac{3\sqrt{8+2\sqrt{28}}}{128}, \tfrac{1+\sqrt{28}}{256} + \tfrac{\sqrt{8+2\sqrt{28}}}{256} \Big\}_{[-4,4]}.$$

Then one can show that a has sum rule order $\mathrm{sr}(a) = 4$, linear-phase moment $\mathrm{lpm}(a * a^\star) = 6$, and $\|a\|_{l_2(\mathbb{Z})} = \frac{\sqrt{25278}}{256}$, $\mathrm{fsp}(a \,|\, \mathrm{hp}) = 4.52\mathrm{e}{-3}$, and $\mathrm{fsp}(a \,|\, \mathrm{lp}) = 4.16\mathrm{e}{-2}$.

Applying Algorithm 1 (S1–S3) with $M = 2$ to split the low-pass filter a, we obtain two auxiliary filters a^+ and a^- with $a^- = \overline{a^+}$, where a^+ is given by $\widehat{a^+}(\xi) := \widehat{a}(\xi)\widehat{u^+}(2\xi)$ with

$$u^+ = \{u^+(k)\}_{k\in[0,2]} = \{(7.13\mathrm{e}{-1}),\ -(5.37\mathrm{e}{-2}) - (6.97\mathrm{e}{-1})i, -(5.50\mathrm{e}{-2})i\}_{[0,2]}.$$

Then $\mathrm{fsp}(a^+) = \mathrm{fsp}(a^-) = 3.32\mathrm{e}{-1}$, $\|a^+\|_{l_2(\mathbb{Z})} = \|a^-\|_{l_2(\mathbb{Z})} = 4.39\mathrm{e}{-1}$.

Applying Algorithm 1 (S4–S5) with $N = 4$, we obtain finitely supported filters b_1^+, b_2^+, b_1^- and b_2^- with $b_1^- := \overline{b_1^+}$ and $b_2^- := \overline{b_2^+}$, where

$$\begin{aligned} b_1^+ = \{&(1.74\mathrm{e}{-2}) - (9.69\mathrm{e}{-3})i, (6.49\mathrm{e}{-2}) + (5.69\mathrm{e}{-2})i, \\ &(3.83\mathrm{e}{-2}) - (1.24\mathrm{e}{-1})i, -(1.29\mathrm{e}{-1}) - (6.07\mathrm{e}{-2})i, \\ &-(7.02\mathrm{e}{-2}) + (1.20\mathrm{e}{-1})i, (6.84\mathrm{e}{-2}) + (1.12\mathrm{e}{-1})i, \\ &(1.05\mathrm{e}{-1}) - (8.18\mathrm{e}{-2})i, -(5.60\mathrm{e}{-2}) - (7.21\mathrm{e}{-2})i, \\ &-(5.99\mathrm{e}{-3}) + (3.99\mathrm{e}{-2})i, (1.54\mathrm{e}{-2}) - (7.13\mathrm{e}{-3})i, \\ &-(6.77\mathrm{e}{-3}) + (3.34\mathrm{e}{-3})i, -(5.88\mathrm{e}{-3}) + (2.85\mathrm{e}{-3})i, \\ &-(1.13\mathrm{e}{-3}) + (5.48\mathrm{e}{-4})i, \\ b_2^+ = \{&-(3.58\mathrm{e}{-2}) - (6.86\mathrm{e}{-3})i, (9.26\mathrm{e}{-2}) + (7.16\mathrm{e}{-2})i, \\ &-(4.13\mathrm{e}{-2}) - (1.88\mathrm{e}{-1})i, -(1.05\mathrm{e}{-1}) + (2.16\mathrm{e}{-1})i, \\ &(1.89\mathrm{e}{-1}) - (1.17\mathrm{e}{-1})i, -(1.62\mathrm{e}{-1}) - (8.41\mathrm{e}{-3})i, \\ &(6.40\mathrm{e}{-1}) + (6.34\mathrm{e}{-2})i, (8.51\mathrm{e}{-3}) - (7.80\mathrm{e}{-3})i, \\ &(7.32\mathrm{e}{-3}) - (4.87\mathrm{e}{-2})i, -(2.41\mathrm{e}{-2}) + (2.72\mathrm{e}{-2})i, \\ &(2.08\mathrm{e}{-3}) + (1.63\mathrm{e}{-3})i, (4.06\mathrm{e}{-3}) - (2.18\mathrm{e}{-3})i, \\ &(7.82\mathrm{e}{-4}) - (4.20\mathrm{e}{-4})i\}_{[-4,8]}. \end{aligned}$$

Then $\mathbb{C}\mathrm{TF}_6 = \{a^+, a^-; b_1^+, b_2^+, b_1^-, b_2^-\}$ is a tight framelet filter bank with $\mathrm{fsp}(b_1^+) = \mathrm{fsp}(b_1^-) = 4.93\mathrm{e}{-2}$, $\mathrm{fsp}(b_2^+) = \mathrm{fsp}(b_2^-) = 1.58\mathrm{e}{-1}$, $\|b_1^+\|_{l_2(\mathbb{Z})} = \|b_1^-\|_{l_2(\mathbb{Z})} = 3.31\mathrm{e}{-1}$, $\|b_2^+\|_{l_2(\mathbb{Z})} = \|b_2^-\|_{l_2(\mathbb{Z})} = 4.44\mathrm{e}{-1}$. The vanishing moments of $b_1^\pm, b_2^\pm$ are $\mathrm{vm}(b_1^+) = \mathrm{vm}(b_1^-) = 3, \mathrm{vm}(b_2^+) = \mathrm{vm}(b_2^-) = 3$. See Figure 1(a)–(b) for the graphs of the frequency separation properties of a^+, b^+, b_1^+, and b_2^+.

V. Numerical Experiments on Image Denoising

In this section, we test the performance of the constructed $\mathrm{cptTP}\text{-}\mathbb{C}\mathrm{TF}_6$ for the image denoising. We compare the performance with its band-limited counterpart $\mathrm{TP}\text{-}\mathbb{C}\mathrm{TF}_6$ as well as several other frame-based methods such as curvelets and shearlets. See [4], [6], [11], [15], [19], [20], [23] on tight wavelet frames and see [1]–[3], [7], [8], [17], [18], [21], [22] for curvelets and shearlets as well as their applications. See

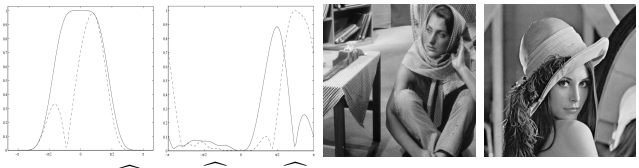

(a) $|\widehat{a}|$ and $|\widehat{a^+}|$ (b) $|\widehat{b_1^+}|$ and $|\widehat{b_2^+}|$ (c) *Barbara* (d) *Lena*

Fig. 1. The frequency separation properties of filters in Example 1 on the basic interval $[-\pi, \pi]$: (a) $|\widehat{a}|$ (solid line) and $|\widehat{a^+}|$ (dashed line). (b) $|\widehat{b_1^+}|$ (solid line) and $|\widehat{b_2^+}|$ (dashed line). (c) Barbara. (d) Lena.

[13], [14], [16], [25] for detail comparison results on the performance of band-limited TP-$\mathbb{C}\mathrm{TF}_n$ with several other transform-based methods. The state-of-the-art BM3D [5] method is also reported here for comparison. Note that BM3D uses more sophisticated block matching techniques for sparse representation which is quite different to other frame-based methods here.

The testing images *Barbara* and *Lena* are given in Figure 1(c)–(d) and all of them are 512×512 gray-scale images. As usual, we use peak signal-to-noise ratio (PSNR) to measure the quality of image restoration. All parameters for the cptTP-$\mathbb{C}\mathrm{TF}_6$ such as level of decomposition, window size in bivariate shrinkage [24], etc., are the same as those of TP-$\mathbb{C}\mathrm{TF}_6$ in [14]. The image denoising experimental setting is same as in [14]; see [14, Section 4] for the details. The comparison results are reported in Table I.

1	2	3	4	5	6
σ	cptTP-$\mathbb{C}\mathrm{TF}_6$ Example 1	TP-$\mathbb{C}\mathrm{TF}_6$ [13], [14]	CurveLab [2]	DNST [22]	BM3D [5]
	512×512 Lena				
5	38.38	38.37	35.77	38.22	38.72
10	35.49	35.48	33.37	35.19	35.93
25	31.57	31.60	30.07	31.09	32.08
40	29.47	29.52	28.15	28.92	29.86
50	28.47	28.54	27.19	27.89	29.05
80	26.40	26.47	25.16	25.71	26.97
100	25.45	25.52	24.22	24.67	25.95
	512×512 Barbara				
5	37.76	37.84	33.83	37.76	38.31
10	34.12	34.18	29.17	33.94	34.98
25	29.37	29.35	24.83	28.90	30.72
40	26.87	26.86	23.87	26.36	27.99
50	25.72	25.71	23.38	25.22	27.23
80	23.52	23.53	22.22	23.11	24.79
100	22.62	22.64	21.61	22.23	23.62

TABLE I
IMAGE DENOISING COMPARISON RESULTS IN TERMS OF PSNR.

In conclusion, the proposed cptTP-$\mathbb{C}\mathrm{TF}_6$ leads to efficient computational algorithm, nice space–frequency localization property, and good performance in image denoising. The combination of block matching techniques and our cptTP-$\mathbb{C}\mathrm{TF}_6$ might lead to improvement of the denoising results. In view of the tensor product nature, such complex tight framelets cptTP-$\mathbb{C}\mathrm{TF}_6$ can be easily extended to any dimension and applied to high-dimensional problems, e.g., video denoising/inpainting. Moreover, thanks to their compactly supported property, the compactly supported complex tight framelets provide the possibility to build directional representation systems on bounded domains, which are important in numerical solutions of partial differential equations. Further development (more theoretical results and examples) and applications (in denoising and inpainting) of cptTP-$\mathbb{C}\mathrm{TF}_n$ will be reported elsewhere.

ACKNOWLEDGMENTS

Research of B. Han was supported in part by the Natural Sciences and Engineering Research Council of Canada (NSERC Canada) under Grant 05865. Research of X. Zhuang was supported in part by Research Grants Council of Hong Kong (Project No. CityU 11302218).

REFERENCES

[1] B. G. Bodmann, G. Kutyniok, and X. Zhuang, Gabor shearlets, *Appl. Comput. Harmon. Anal.* **38**(1)(2015), 87–114.
[2] E. J. Candès, L. Demanet, D. L. Donoho, and L. Ying, Fast discrete curvelet transforms, *Multiscale Model. Simul.* **5**(3)(2006), 861–899.
[3] Z. Che and X. Zhuang, Digital affine shear filter banks with 2-Layer structure and their applications in image processing, *IEEE Trans. Image Process.* **27**(8)(2018), 3931 – 3941.
[4] C. K. Chui, W. He, and J. Stöckler, Compactly supported tight and sibling frames with maximum vanishing moments, *Appl. Comput. Harmon. Anal.* **13**(3)(2002), 224–262.
[5] K. Dabov, A. Foi, V. Katkovnik, and K. Egiazarian, Image denoising by sparse 3D transform-domain collaborative filtering, *IEEE Trans. Image Process.* **16**(8)(2007), 2080–2095.
[6] I. Daubechies, B. Han, A. Ron, and Z. Shen, Framelets: MRA-based constructions of wavelet frames, *Appl. Comput. Harmon. Anal.* **14**(1)(2003), 1–46.
[7] G. Easley, D. Labate, and W. Lim, Sparse directional image representations using the discrete shearlet transform, *Appl. Comput. Harmon. Anal.* **25**(2008), 25–46.
[8] K. Guo, G. Kutyniok, and D. Labate, *Sparse multidimensional representations using anisotropic dilation and shear operators*, Wavelets and Splines (Athens, GA, 2005), Nashboro Press, Nashville, TN (2006), 189–201.
[9] B. Han, Nonhomogeneous wavelet systems in high dimensions, *Appl. Comput. Harmon. Anal.* **32**(2)(2012), 169–196.
[10] B. Han, Properties of discrete framelet transforms, *Math. Model. Nat. Phenom.* **8**(1)(2013), 18–47.
[11] B. Han, *Framelets and Wavelets: Algorithms, Analysis, and Applications*. Springer International Publishing, 2018.
[12] B. Han, Q. Mo, and Z. Zhao, Compactly supported tensor product complex tight framelets with directionality, *SIAM J. Math. Anal.* **47**(3)(2015), 2464–2494.
[13] B. Han and Z. Zhao, Tensor product complex tight framelets with increasing directionality, *SIAM J. Imaging Sci.* **7**(2)(2014), 997–1034.
[14] B. Han, Z. Zhao, and X. Zhuang, Directional tensor product complex tight framelets with low redundancy, *Appl. Comput. Harmon. Anal.* **41**(2)(2016), 603–637.
[15] B. Han and X. Zhuang, Algorithms for matrix extension and orthogonal wavelet filter banks over algebraic number fields, *Math. Comput.* **82**(281)(2013), 459–490.
[16] B. Han and X. Zhuang, Smooth affine shear tight frames with MRA structure, *Appl. Comput. Harmon. Anal.* **39**(2015), 300–338.
[17] G. Kutyniok and D. Labate, Shearlets: Multiscale Analysis for Multivariate Data, Birkhäuser, 2012.
[18] G. Kutyniok, M. Shahram, and X. Zhuang, ShearLab: a rational design of a digital parabolic scaling algorithm, *SIAM J. Imaging Sci.* **5**(2012), 1291–1332.
[19] Y.-R. Li, R. H. Chan, L. Shen, Y.-C. Hsu, and W.-Y. Tseng, An adaptive directional Haar framelet-based reconstruction algorithm for parallel magnetic resonance imaging. *SIAM J. Imaging Sci.* **9**(2016), 794–821.
[20] Y.-R. Li, L. Shen, and B. W. Suter, Adaptive inpainting algorithm based on DCT induced wavelet regularization, *IEEE Trans. Image Process.* **22**(2)(2013), 752–763.
[21] W.-Q Lim, The discrete shearlet transform: a new directional transform and compactly supported shearlet frames, *IEEE Trans. Image Process.* **19**(5)(2010), 1166–1180.

[22] W.-Q Lim, Nonseparable shearlet transform, *IEEE Trans. Image Process.* **22**(5)(2013), 2056–2065.
[23] A. Ron and Z. Shen, Affine systems in $L_2(\mathbb{R}^d)$: the analysis of the analysis operator, *J. Funct. Anal.* **148**(1997), 408–447.
[24] L. Sendur and I. W. Selesnick, Bivariate shrinkage with local variance estimation, *IEEE Signal Process. Letters*. **9**(2002), 438–441.
[25] Y. Shen, B. Han, and E. Braverman, Image inpainting from partial noisy data by directional complex tight framelets, *ANZIAM*. **58**(2017), 247–255.